AGU ADVANCING EARTH AND SPACE SCIENCE

Geophysical Research Letters®

RESEARCH LETTER
10.1029/2021GL095305

Nitrous Oxide Emissions From Drying Streams and Rivers

D. Tonina[1], A. Marzadri[2], A. Bellin[2], M. M. Dee[3], S. Bernal[4], and J. L. Tank[5]

[1]Center for Ecohydraulics Research, University of Idaho, Boise, ID, USA, [2]Department of Civil, Environmental and Mechanical Engineering, University of Trento, Trento, Italy, [3]Michigan Sea Grant, Michigan State University Extension, East Lansing, MI, USA, [4]Centre d'Estudis Avançats de Blanes -Consejo Superior de Investigaciones Cientificas (CEAB-CSIC), Barcelona, Spain, [5]Department of Biological Sciences, University of Notre Dame, Notre Dame, IN, USA

Abstract Streams and rivers are suffering more extreme and prolonged low flows than those naturally occurring without human intervention with potential relevant worldwide effects on the production of nitrous oxide (N_2O), a greenhouse gas 300 times more potent than carbon dioxide. Here, we address the question of whether droughts and management-induced low flows increase riverine N_2O emissions causing positive feedback in response to climate change. Supported by field data, we model riverine N_2O emissions for decreasing mean summer flows in a forested and agricultural watershed under chemostatic and chemodynamic dissolved inorganic reactive nitrogen (DIN) concentrations. Our results demonstrate that total N_2O emissions decrease with increasing low flow severity in both watersheds regardless of DIN scenario; which imparts a form of climate resilience.

Plain Language Summary Emissions of the ozone-layer destructor and potent greenhouse gas nitrous oxide, N_2O, from rivers are a function of both nitrate loads and stream flows. Here we answer the question of whether droughts and subsequent low flows may exacerbate climate change by increasing N_2O emissions, thus forming positive feedback, which may self-reinforce the adverse effects of climate change. We demonstrate that total N_2O emissions may remain similar or decrease with decreasing flows in both agricultural and forested watersheds. The reduction is mainly due to reduced water surface areas. However, N_2O emissions per stream water surface unit area significantly increase in agricultural reaches due to both high nitrate concentrations and their morphological characteristics but remain constant or decrease in reaches flowing in forested watersheds.

Key Points:

- Low flows lead to higher N_2O emission per unit stream area in agricultural but not in forested reaches
- Total riverine N_2O emissions decrease with low flow severity regardless of land use
- Increasing low flow severity does not induce positive feedback to climate change due to N_2O emissions

Supporting Information:

Supporting Information may be found in the online version of this article.

Correspondence to:

D. Tonina,
dtonina@uidaho.edu

Citation:

Tonina, D., Marzadri, A., Bellin, A., Dee, M. M., Bernal, S., & Tank, J. L. (2021). Nitrous oxide emissions from drying streams and rivers. *Geophysical Research Letters*, *48*, e2021GL095305. https://doi.org/10.1029/2021GL095305

Received 30 JUL 2021
Accepted 3 DEC 2021

Author Contributions:

Conceptualization: D. Tonina, A. Marzadri, A. Bellin, M. M. Dee, J. L. Tank
Data curation: A. Marzadri, M. M. Dee
Formal analysis: D. Tonina, A. Marzadri, A. Bellin, M. M. Dee
Funding acquisition: D. Tonina, A. Bellin, J. L. Tank
Investigation: A. Marzadri, M. M. Dee, S. Bernal, J. L. Tank
Project Administration: D. Tonina, A. Bellin, J. L. Tank
Resources: J. L. Tank
Software: A. Marzadri
Validation: A. Marzadri
Visualization: D. Tonina, A. Marzadri
Writing – original draft: D. Tonina

1. Introduction

Streamflow, along with land use practices (e.g., agriculture), are important determinants of the export of carbon (Hotchkiss et al., 2015), nutrients (Rinaldo et al., 2006) and contaminants (Kaushal et al., 2014; Vidon & Cuadra, 2010) along riverine networks. In addition, low flows (i.e., discharges below the base flow, which is the flow other than runoff sustained primarily by springs and groundwater seepage, Smakhtin, 2001 and Supporting Information S1), caused by droughts or water uses (Miller et al., 2021), may influence stream biogeochemical processes, as well as the transformation and uptake of dissolved solutes. Drought is a significant stressor in agricultural lands, with significant socioeconomic implications (Overpeck, 2013; Sheffield et al., 2014), as well as direct impacts on the amount and timing of solutes and particles lost from landscapes to waterways. Among the dissolved constituents, dissolved reactive inorganic nitrogen (DIN), especially nitrate (NO_3^-), plays an important role at the global scale. Because it fuels the emission of nitrous oxide N_2O (Seitzinger et al., 2000) from riverine systems via the process of microbially-mediated denitrification (Beaulieu et al., 2011; Seitzinger, 1988). Moreover, N_2O is a potent greenhouse gas that is also responsible for stratospheric ozone destruction (Ravishankara et al., 2009). However, limited research has examined N_2O emissions from streams and rivers during low flow conditions (Audet et al., 2017). Even fewer studies have provided emission predictors at ecologically relevant scales (Baulch et al., 2011; Marzadri et al., 2017; Turner et al., 2015), due to the difficulties in upscaling local processes occurring in the hyporheic zone (subsurface streambed sediment), benthic zone (sediment-water surface), and water column, to the scale of river networks. We do not know whether N_2O emissions will increase or decrease as river and stream flows (i.e., discharge) decrease below normal base flows, which will be critical in assessing the feedback between predicted impacts of climate change and N_2O emissions from riverine systems. Low flows may exacerbate the effects of climate change, via a positive feedback in which extended low flow conditions increases N_2O emissions, or attenuate drought effects due to reduction in N_2O emissions, depending

Writing – review & editing: D. Tonina, A. Marzadri, A. Bellin, M. M. Dee, S. Bernal, J. L. Tank

on local land cover, water use, and changes in surface hydraulics (Marzadri et al., 2017). River morphology may change with discharge, for instance, dune size adjusts to local discharge because fine sediments are typically mobile even at low flows (Yalin, 1964). These morphological changes, in turn, impact hyporheic hydraulics and thus the time for biogeochemical transformation within streambeds. Moreover, nutrient concentrations may be discharge-dependent or behave as chemostatic (similar concentration regardless of discharge) depending on land uses (Basu et al., 2010; Levi et al., 2018). Denitrification reaction rate constant also changes depending on both solute concentration and surface hydraulics (see, Supporting Information S1 and Beaulieu et al., 2011; Davis & Minshall, 1999; Mulholland et al., 2008). These complex dependence of N_2O emissions on local processes, from river morphology to biological reactivity, hinder predicting N_2O emissions with decreasing discharge and prevent simple extrapolation of N_2O trends observed under natural base flows to more extreme low flows conditions.

Here, we used the N_2O emission model developed by Marzadri et al. (2017) and successively modified by Marzadri et al. (2021), which accounts for biological processing within the riverine hyporheic benthic and water column environments, to identify the hydrological and environmental conditions that cause riverine systems to increase or decrease total N_2O emissions during low flows, at areal and whole-river network scales. We applied the model to two low-gradient watersheds with contrasting land-use land-cover: the Manistee River (Michigan, USA; ~83% forested) and the Tippecanoe River (Indiana, USA; ~82% agricultural). We collected two sets of 80 synoptic samples, providing water temperature and concentrations of NO_3^-, N_2O, and ammonium (NH_4^+), across both watersheds during a typical base flow condition during summer 2015. These model input data were supplemented by hydro-morphological measurements, including mean flow depth, velocity, width, substrate size, and bedform type at the same synoptic sites, thereby allowing the model to account for changes in stream hydraulics and morphology as discharge changes (Stewart et al., 2011) (see Supporting Information S1).

2. Methods

The Marzadri et al. (2021) model does not require calibration to predict the dimensionless N_2O flux (F^*N_2O) and it is fully characterized by reach-scale, hydro-morphological characteristics, such as roughness, streambed morphology and discharge, and how these metrics change as a function of flow regime, combined with stream water temperature, and stream dissolved inorganic nitrogen (DIN) concentrations (see Supporting Information S1). F^*N_2O represents a type of N_2O emission factor, at the reach scale resolution (Marzadri et al., 2021), and is defined as the ratio between the flux of N_2O (FN_2O) per unit stream area and the in-stream flux of DIN species per unit stream cross-section area (NH_4^+ and NO_3^-; $FDIN = V\cdot([NO_3^-] + [NH_4^+])$, with V as the mean reach flow velocity. F^*N_2O value depends on the dimensionless Damköhler number, Da_D, which accounts for reach-scale hydro-morphological and biochemical characteristics. The Da_D is defined as the ratio between the residence time τ in the compartment where denitrification chiefly occurs and the characteristic time of denitrification τ_D: $Da_D = \tau/\tau_D$. Two relevant stream compartments are considered: (a) the hyporheic zone, including the overlying benthic zone, with a characteristic residence time defined as the median of the travel time within the hyporheic zone τ_{50}, and (b) the water column, with a characteristic time identifiable as the turbulent vertical mixing time scale $t_m = D/(0.067[g\cdot D\cdot s_0]^{0.5})$, where g is the gravitational acceleration, D is the mean flow depth and s_0 is the friction slope (Rutherford, 1994). In small systems (i.e., streams), denitrification occurs chiefly in the benthic-hyporheic zone, but as systems widen (i.e., in rivers) and their slope declines, water depth increases and denitrification occurs mostly in the water column. These two situations are represented by using two different Da_D numbers: $Da_{DHZ} = \tau_{50}/\tau_D$ for headwater streams, and $Da_{DS} = t_m/\tau_D$ for rivers. River morphology (dunes but not pool-riffle, whose size depends on effective discharge [e.g., Tubino, 1991]) and local hydraulics are dynamically linked to discharge such that the model can account for direct impact of discharge to flow regime, and indirectly on stream bedform size (see Supporting Information S1). For both Da_D numbers, the biological processes are represented via the denitrification time scale, τ_D, which is the inverse of the denitrification reaction rate and is quantified as a function of the stream denitrification uptake rate, v_{fden} (see Supporting Information S1). The v_{fden} is a mass transfer coefficient, which is operationally defined as "demand relative to concentration" and its value decreases as NO_3^- concentrations increase (Davis & Minshall, 1999) typically in the form of $v_{fden} = a\cdot[NO_3^-]^b$ with a and b being regression coefficients (Beaulieu et al., 2011; Mulholland et al., 2008).

The model consists of three equations, whose application depends on stream size, expressed as channel width, W, because the main source of N_2O emissions shifts from the hyporheic zone in small streams (HZ Model), chiefly benthic zone for intermediate streams (BZ Model) and then to the water column for rivers (WC Model):

$$\begin{cases} \text{HZ}: \quad F^*N_2O_{HZ} = 1.55 \cdot 10^{-7}(Da_{DHZ})^{0.43}, \ (r^2 = 0.48), & W \le 10 \text{ m} \\ \text{BZ:} F^*N_2O_{BZ} = 1.91 \cdot 10^{-8}(Da_{DHZ})^{0.57}, \ (r^2 = 0.40), & 10 \text{ m} < W \le 175 \text{ m} \\ \text{WC}: \ F^*N_2O_{WC} = 4.56 \cdot 10^{-6}(Da_{DS})^{0.72}, \ (r^2 = 0.54), & W > 175 \text{ m} \end{cases} \quad (1)$$

Marzadri et al. (2017) derived the first two equations (Equation 1 $F^*N_2O_{HZ}$ and $F^*N_2O_{BZ}$) by using a mechanistic model of emissions applied to the data collected in 12 stream reaches of the Kalamazoo (MI, USA) (Beaulieu et al., 2008, 2009) and 16 reaches from the second iteration of the Lotic Intersite Nitrogen eXperiment (LINXII) (Beaulieu et al., 2011; Hall et al., 2009; Mulholland et al., 2008). The obtained equations were validated against measured emissions from 400 reaches of streams and rivers worldwide during summer base flows with riverine water temperatures ranging between 11 and 36°C. The third equation of the model ($F^*N_2O_{WC}$) was obtained analyzing measured emissions from streams and rivers with width larger than 30 m in terms of the Damköhler number that considers the major role played by the water column in controlling emissions (Da_{DS}); this is expressed differently from the first two equations and is a regression-based model that we validated with independent data (Figure S1 in Supporting Information S1).

Stream N_2O measurements along with hydro-morphological data collected during drought conditions are scarce. To our knowledge, we collected and used all those measurements available in the literature: nine headwater streams from a small Swedish agricultural catchment (C6, Kyllmar et al., 2006; Figure S2 in Supporting Information S1) and eight reaches of the San Joaquin River (Hinshaw & Dahlgren, 2012). The performance of HZ model in predicting N_2O emissions during low flow conditions was tested with the data from the Swedish streams ($r^2 = 0.53$, Figure S3 in Supporting Information S1), and that of the BZ model with the data from San Joaquin River ($r^2 = 0.43$, Figure S3 in Supporting Information S1). In the two cases, only reaches within the HZ ($W \le 10$ m) and BZ bounds ($W > 30$ m) were included in the analysis.

We quantified the role of low flows in N_2O emissions by applying the above framework to the Manistee River (MI, USA, forested) and the Tippecanoe River (IN, USA, agricultural). The Manistee River is forested over 83% of its 3,616 km^2 watershed, stream flow discharges range between 22 and 14,000 L/s and summer low-flow NO_3^- concentrations average 120 µg N/L. The Tippecanoe River has 82% of its 4,496 km^2 basin in row-crop agriculture, discharges range between 0.9 L/s and 22,500 L/s and summer low-flow NO_3^- concentrations average 1,860 µg N/L. Both watersheds have reaches with dune-like or pool-riffles morphologies with sediments composed by gravel and sand. Information from the grain size distribution allowed estimation of the hydraulic conductivity of the streambed sediment (Salarashayeri & Siosemarde, 2012).

We collected all the required hydro-morphological and water quality information during a synoptic sampling effort in summer 2015, at 80 locations in each watershed, collected within a 24-hr period, at baseflow conditions. To apply the model to each reach of the riverine network, we spatially distributed these original measurements of temperature, NH_4^+ and NO_3^- concentrations along the two riverine networks using the Spatial Stream Network (SSN; R) (Ver Hoef et al., 2014) model and Spatial Tools for the Analysis of River Systems (STARS; ArcGIS) (Peterson & Ver Hoef, 2014), which uses a one-dimensional geostatistical interpolation along the streams. Mean flow velocity, depth and width were spatially distributed with a set of regime equations developed from the 80 locations at each watershed (Equations S9 and S10 in Supporting Information S1). Bedform type and size were derived by combining Montgomery and Buffington stream classification (Montgomery & Buffington, 1998) with hydro-morphological relationships for dune and pool-riffle. Bedform prediction was verified with visual inspection at the sites. Stream discharge was predicted at each reach of the river networks with the GIS tools ArcHydro and Hec-GeoHMS, which provided the input conditions for the Land Surface Model (Piccolroaz et al., 2016) that predicted the lateral inflows to the river network. Flow generation was accomplished with a continuous soil-moisture accounting model based on the SCS-CN methodology (Avesani et al., 2021). Stream flows were then routed with a validated (averaged Nash-Sutcliffe index larger than 0.7) Muskingum flow routing scheme (Cunge, 1969) at the reach scale.

The resolution of the model and input data allows us to explore the response of N_2O emissions longitudinally, from headwaters to mainstem reaches, along the forested and agriculture watershed, and at the watershed scale under different scenarios of decreasing low flows (i.e., increasing drought severity). The mean daily discharge (Q_{sum}) in summer is a common statistic used for water resource planning with important ecological and water use implications (WMO, 2008). Thus, we used Q_{sum} as our reference discharge for current flows and selected three

alternative mean summer flows, which may replace the current Q_{sum} in future scenarios resulting from climate-induced increase in drought severity or low flows induced by water uses. These data represent current daily base flow conditions, and their 25th and 5th percentiles, which we quantify from daily discharges monitored at six US Geological Survey (USGS) gauging stations located within the two watersheds with the R package lfstat (Koffler & Laaha, 2012). We define these three alternative summer mean flows as moderate low Q_{sum}, very low Q_{sum}, and extremely low Q_{sum}. Current information on DIN concentration and temperature distributions were then used as reference values for simulating N_2O fluxes. We considered the two most likely end member scenarios for FDIN: constant DIN concentrations (i.e., chemostatic scenario) and constant FDIN (i.e., conservation of mass flux, chemodynamic scenario) (Basu et al., 2010; Levi et al., 2018). In chemostatic scenario, a flow reduction gives rise to a contemporaneous reduction in catchment inputs (Mosley, 2015) and thereby a reduction of FDIN (see example, Figure S4a in Supporting Information S1). However, in chemodynamic scenario, an increase in DIN concentrations may offset the lower flows resulting in a constant FDIN, rather than constant DIN concentrations, with decreasing discharge (Hinshaw & Dahlgren, 2012) (see example, Figure S4b in Supporting Information S1).

Total N_2O emissions (TE) at the watershed scale were quantified at daily time steps with:

$$TE = \sum_{r=1}^{Nr} F^*N_2O_r \cdot FDIN_r \cdot W_r \cdot L_r \quad (2)$$

where N_r is the number of the reaches that compose the stream network, W_r is the width of the r-th reach, L_r is its length, $F^*N_2O_r$ is its dimensionless N_2O emission estimated with the power law scaling model (Equation 1), and $FDIN_r$ is its flux of DIN.

3. Results and Discussion

The effect of the DIN scenario considered on F^*N_2O was large because DIN concentration influenced the calculation of Da_D via v_{fden}. For the chemodynamic scenario, F^*N_2O values remained almost constant (Figure S5 in Supporting Information S1), while values increased for the chemostatic scenario. In the latter case, the model predicted a statistically significant increase in F^*N_2O with lower flows in the agricultural headwater (HW, stream orders 1 to 3) and main stem (MS, stream order >3) reaches, but not for the forested headwater and mainstem reaches (Figure 1; Kruskal-Wallis non-parametric test results in Table S4 in Supporting Information S1). The impact of low flows on F^*N_2O in agricultural reaches reflects its land use footprint characterized by narrower streams (including ditches) compared to the forested watershed (Figure S5 in Supporting Information S1). As such, the hydro-morphological characteristics especially in HW are more sensitive to changes in discharge in the agricultural than in the forested watershed, as indicated by the 30% decline in mean W simulated for extreme low Q_{sum} (Figures S6 in Supporting Information S1). In contrast, forested HW streams have a less pronounced reduction in width (half of the agricultural, 15%) and smaller changes in Damkhöler numbers (1.4% increase) with low-flow severity than the agricultural HW, which shows a 26% increase in Damkhöler numbers (Figures S6 and S7 in Supporting Information S1). In contrast to HW, simulated low flow conditions have subtler impacts on main stem hydromorphology (e.g., mean W reductions of 7% and 13% from Q_{sum} to extreme low Q_{sum} for the forested and agricultural MS, respectively), which drives the non-significant changes in F^*N_2O in river forested MS, but still significant in the agricultural.

However, an increase in F^*N_2O does not necessarily lead to an increase of FN_2O from riverine systems, because changes in FN_2O depend also on DIN availability (FDIN), which is influenced by land use, land cover, and discharge (Basu et al., 2010; Marinos et al., 2020; Mosley, 2015). Both FDIN scenarios did not significantly change FN_2O in either HW or MS reaches in the forested watershed. Conversely, the chemodynamic scenario caused significant increase of FN_2O with decreasing low flows in the agricultural HW reaches, whereas the chemostatic scenario caused a significant reduction in FN_2O with low flow severity in the agricultural MS reaches (Figure 1 and Kruskal-Wallis test results in Table S4 in Supporting Information S1).

We found that the distribution of DIN concentrations measured during the summer synoptic sampling showed a clustering of high and low concentrations within sub-basins, rather than a longitudinal pattern from headwater to mainstem reaches (Figures 2a and 2b). As such, the change in N_2O emissions per unit streambed area (ΔFN_2O) induced by the extreme low flow scenario showed a systematic decrease from HW to MS reaches (except for order 1), suggesting that low flows accentuate increases in FN_2O from headwater reaches, especially from stream

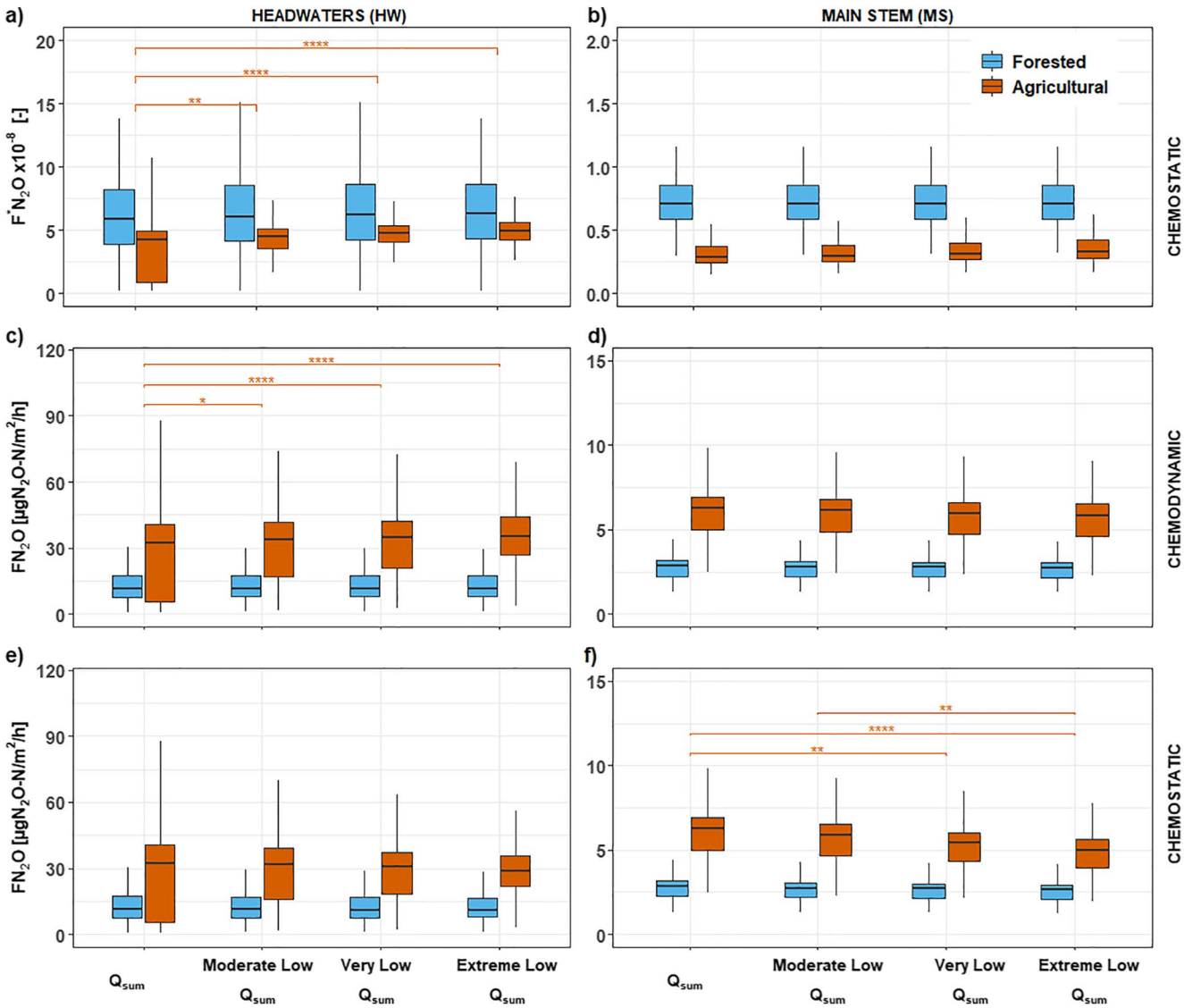

Figure 1. Box plot (15th, 50th and 75th quartiles with the 10% and 90% within the whiskers) of N_2O emissions from forested (light blue fill) and agricultural (red fill) reaches. The scale of the *Y*-axis changes among panels to better present the data. The top panels (a) and (b) show the dimensionless areal emission F^*N_2O for the chemostatic case, whereas the middle and bottom panels show the actual areal emission FN_2O for constant FDIN (conservation of mass flux, i.e., chemodynamic scenario) (c) and (d), and constant DIN concentrations (chemostatic FDIN scenario) (e) and (f) from headwaters (HW, left panels) and the mainstem (MS, right panels). Brackets report the *p* value significance (*$p < 0.05$, **$p < 0.01$, ***$p < 0.001$ and ****$p < 0.0001$) of the statistically significant changes in F^*N_2O and FN_2O with low flow severity with the non-parametric Wilcoxon test. If not reported the trend is not statistically significant. Only the agricultural watershed has some scenarios with statistically significant changes: F^*N_2O from headwaters and mean stems for the chemostatic scenario and FN_2O from headwaters for the chemodynamic scenario significantly increase with increasing low flow severity, but FN_2O values decrease for the main stems with the chemostatic scenario (also see Kruskal-Wallis test in Table S4 in Supporting Information S1).

orders 2 and 3 (Figures 2g and 2h). The same results were found for total emissions quantified from headwater or mainstream reaches, which further underscores the importance of headwater streams in controlling N_2O emissions at the watershed scale (Table S5 in Supporting Information S1). We found that this pattern was accentuated in agricultural reaches compared to forested ones (Figures 2c, 2h and Figure S8 in Supporting Information S1), likely because the former had a stronger reduction in width, which contributed to decrease FN_2O (Figure S6 in Supporting Information S1). This size change is critical because the hyporheic zone is the dominant source of N_2O yield in HW streams, but its role decreases rapidly as size increases, from HW to MS.

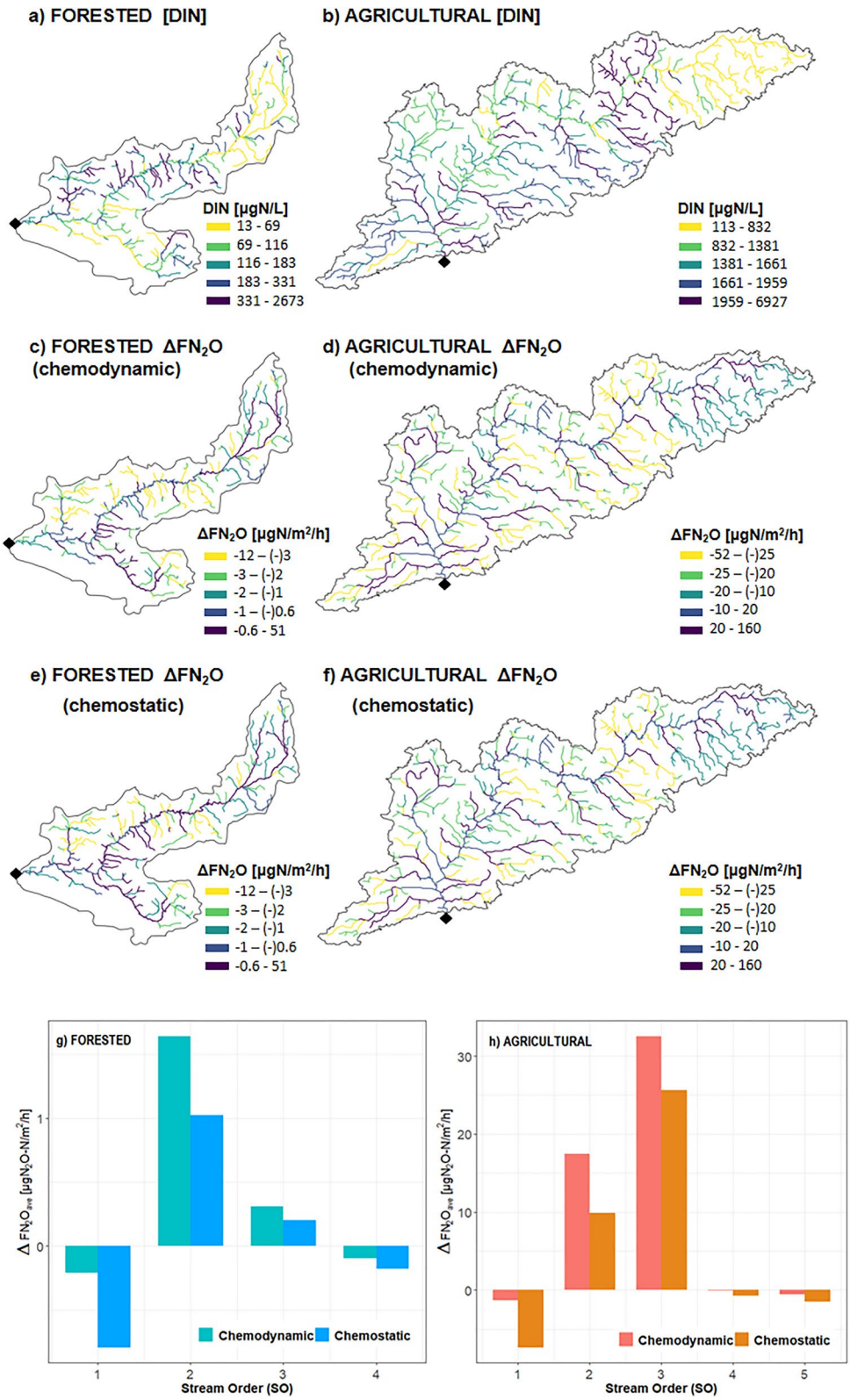

Figure 2. In-stream dissolved inorganic nitrogen concentration (DIN) distributions derived from the 2015 summer synoptic measurements along the forested (a) and the agricultural (b) watersheds, and distribution of differences, ΔFN_2O, between FN_2O for extreme low and current Q_{sum} for constant FDIN (conservation of mass flux, i.e., chemodynamic scenario) (c) and (d), and constant DIN concentrations (chemostatic scenario) (e) and (f), along the forested (right panels) and the agricultural (left panels) watersheds. Histograms of ΔFN_2O as a function of stream order for the forested (g) and agricultural (h) watersheds.

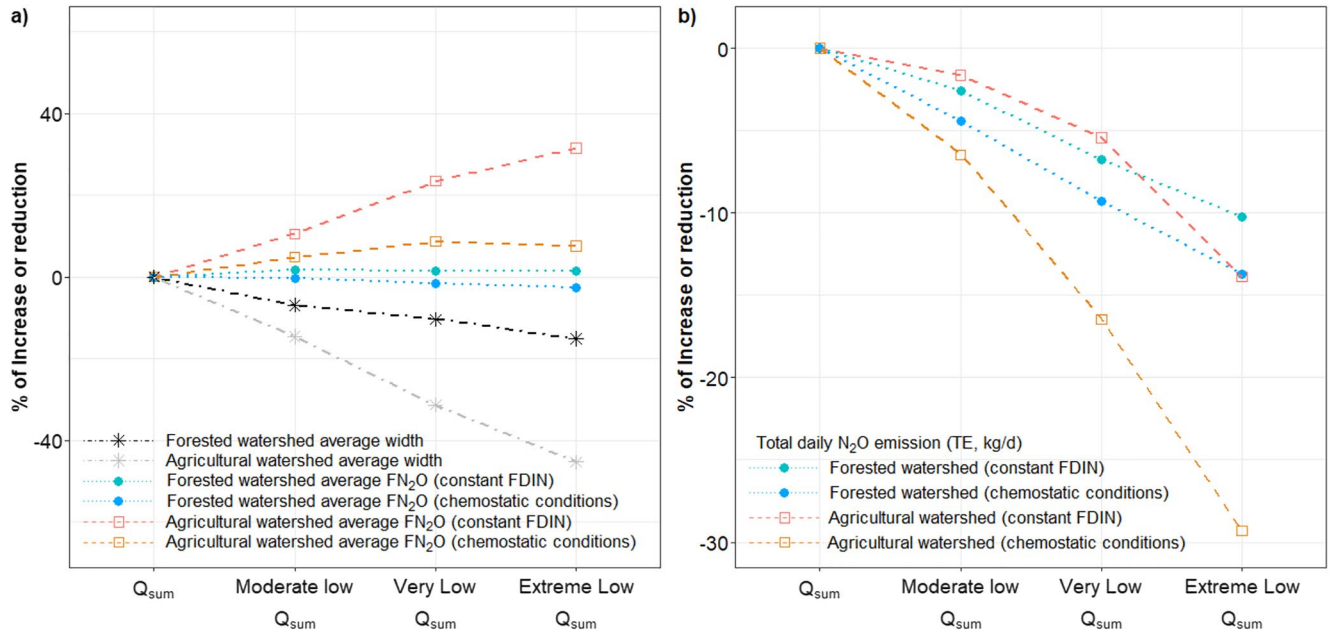

Figure 3. Relative changes in (a) average N_2O flux (FN_2O open squares and solid circles) and average channel width (*W*, star symbols) and (b) total daily emission (TE) of N_2O, for the current, moderate low, very low and extreme low Q_{sum} scenarios for the forested (solid circles) and agricultural (open squares) watersheds for constant FDIN (conservation of mass flux, i.e., chemodynamic scenario) and constant DIN concentrations (chemostatic scenario).

Mean FN_2O increased for the chemodynamic scenario (i.e., constant DIN flux) regardless of watershed type, but FN_2O decreased for the chemostatic case for the forested watershed (Figure 3a). Overall, the FN_2O patterns for the forested watershed showed less dependence on the DIN scenario considered compared to the agricultural watershed, suggesting that forested watersheds are more resilient to increasing the occurrence of low flows.

The spatial distribution of changes in FN_2O demonstrates how biogeochemistry, hydrology, and land use practices interact to influence N_2O emissions from different reaches within a stream network (Figures 2c–2h). However, it is essential to understand the response of entire watersheds to increasing low flow conditions by transitioning N_2O emissions from a reach-to a whole fluvial network-scale perspective. We calculated the total N_2O emissions (TE) over the entire watershed at daily time scale by accounting for each reach surface area (See Equation 2 in Section 2). Whereas average FN_2O may slightly decrease or increase up to 38% depending on the DIN concentration scenario and watershed considered (Figure 3a), channel width, which controls the riverine surface areas (reach length is fixed), is expected to decrease or at the most remain constant with increasing low flow severity (Figure 3a, star symbols). For the three low flow scenarios, the model predicts a decrease in total daily N_2O emissions for both watersheds regardless of the DIN scenario considered (i.e., chemodynamic or chemostatic), primarily driven by the reduction in channel width (Figure 3b).

All scenarios result in a decrease of TE emission between 10% and 20%. The reduction in stream width (grey star symbol Figure 3a) compensate the almost 40% increase in FN_2O (Figure 3a pink square open symbols). This effect is stronger in headwater than main stem reaches (Table S5 in Supporting Information S1). Our analysis indicates that the compensatory role of changes in channel morphology is critical if we are to understand the feedback between climate change and its effect on the biogeochemistry of streams and rivers. Whereas the results obtained at the reach scale may suggest that lower flows, and eventually higher DIN concentrations in headwater reaches, could lead to overall higher N_2O emissions (Figures 2g and 2h and Figure 3a), our watershed-scale analysis points toward the opposite direction: total emissions of N_2O at the watershed scale would likely decrease with increasing drought conditions in the future because reduction in flow and stream width will hold down N_2O emissions even in agricultural watersheds where increases in DIN concentration are expected (Figure 3b).

4. Conclusions

Our results highlight that the impact of drought on N_2O emission factor expressed as F^*N_2O and emissions per unit area of stream (FN_2O) was maximized in headwater reaches but decreased with increasing stream size in the river mainstems. This finding underscores the importance of managing (e.g., DIN runoff and channelization) small headwater streams, especially in agricultural lands. Drought conditions significantly decrease FN_2O in those reaches where no changes in DIN concentration are expected (i.e., chemostatic scenario). Yet, in most stream reaches, the increase in low flow condition (i.e., drought severity) lead to increases in FN_2O for the scenario of future increases in DIN concentrations and constant DIN fluxes, which is the most critical situation in streams draining agricultural lands with long-lasting legacy effects. Conversely, changes in FN_2O are subtle, and not statistically significant for stream reaches at the forested watershed. However, our conclusions on the implications of increasing drought conditions for N_2O emissions drastically change when results are integrated at the whole fluvial network scale because of the interplay between changes in FN_2O and channel width. While FN_2O at the reach scale may increase or decrease with drought conditions, channel width will mostly decrease. The combined effect of these two variables results in an amplified reduction of N_2O emissions from forested and agricultural networks regardless of the DIN scenario. These results stress the intertwined link between in-stream biological processing and hydrological conditions; hydrology does not only control the mean residence time of water, and with that, the Damköhler number and the characteristic time of denitrification, but also drives the expansion and contraction of the fluvial network, which is a fundamental feature for understanding how changes in biogeochemical fluxes per unit stream area resonate at the whole fluvial network scale. Overall, our results show no evidence that climate change-induced drought would cause positive feedback on N_2O emissions, but rather suggests that low flow conditions would contribute to a decrease watershed-scale N_2O emissions in both agricultural and forested landscapes.

Conflict of Interest

The authors declare no conflict of interest relevant to this study.

Data Availability Statement

Data are available at Tonina et al. (2021), http://www.hydroshare.org/resource/70a1078d0ca14839aeea8e0f-4082cb81.

Acknowledgments

This study was partially supported by the NSF awards 1340749 and 1344602. A.B. and A. M. acknowledge funding from the Italian Ministry of Education, University and Research (MIUR) in the frame of the Departments of Excellence Initiative 20182022 granted to the Department of Civil, Environmental and Mechanical Engineering of the University of Trento, D.T. the support from the USDA National Institute of Food and Agriculture, Hatch project 1012806, SB acknowledge funding by the RTI2018-094521-B-100, and RYC-2017-22643 awards from the Spanish Ministry of Science, Innovation, and AEI/FEDER UE. We thank two anonymous reviewers and the Editor for their critical, valuable, and constructive suggestions and comments, which improved the contribution. We also thank Dr Sebastiano Piccolroaz for his support on the hydrological modeling. Any opinions, conclusions, or recommendations expressed in this material are those of the authors and do not necessarily reflect the views of the supporting agencies.

References

Audet, J., Wallin, M. B., Kyllmar, K., Andersson, S., & Bishop, K. (2017). Nitrous oxide emissions from streams in a Swedish agricultural catchment. *Agriculture, Ecosystems & Environment*, *236*, 295–303. https://doi.org/10.1016/j.agee.2016.12.012

Avesani, D., Galletti, A., Piccolroaz, S., Bellin, A., & Majone, B. (2021). A dual-layer MPI continuous large-scale hydrological model including Human Systems. *Environmental Modelling & Software*, *139*, 105003. https://doi.org/10.1016/j.envsoft.2021.105003

Basu, N. B., Destouni, G., Jawitz, J. W., Thompson, S. E., Loukinova, N. V., Darracq, A., et al. (2010). Nutrient loads exported from managed catchments reveal emergent biogeochemical stationarity. *Geophysical Research Letters*, *37*, 1–5. https://doi.org/10.1029/2010GL045168

Baulch, H. M., Schiff, S. L., Maranger, R., & Dillon, P. J. (2011). Nitrogen enrichment and the emission of nitrous oxide from streams. *Global Biogeochemistry*. Cycles 25. https://doi.org/10.1029/2011GB004047

Beaulieu, J. J., Arango, C. P., Hamilton, S. K., & Tank, J. L. (2008). The production and emission of nitrous oxide from headwater streams in the midwestern USA. *Global Change Biology*, *14*, 878–894. https://doi.org/10.1111/j.1365-2486.2007.01485.x

Beaulieu, J. J., Arango, C. P., & Tank, J. L. (2009). The effects of season and agriculture on nitrous oxide production in headwater streams. *Journal of Environmental Quality*, *38*, 637–46. https://doi.org/10.2134/jeq2008.0003

Beaulieu, J. J., Tank, J. L., Hamilton, S. K., Wollheim, W. M., Hall, R. O., Mulholland, P. J., et al. (2011). Nitrous oxide emission from denitrification in stream and river networks. *Proceedings of the National Academy of Sciences of the United States of America*, *108*, 214–219. https://doi.org/10.1073/pnas.1011464108

Cunge, J. A. (1969). On the subject of a flood propagation computation method (Muskingum method). *Journal of Hydraulic Research*, *7*, 205–230. https://doi.org/10.1080/00221686909500264

Davis, J. C., & Minshall, G. W. (1999). Nitrogen and phosphorus uptake in two Idaho (USA) headwater wilderness streams. *Oecologia*, *119*, 247–255. https://doi.org/10.1007/s004420050783

Hall, R. O., Tank, J. L., Sobota, D. J., Mulholland, P. J., O'Brien, J. M., Dodds, W. K., et al. (2009). Nitrate removal in stream ecosystems measured by N-15 addition experiments: Total uptake. *Limnology & Oceanography*, *54*, 653–665. https://doi.org/10.4319/lo.2009.54.3.0653

Hinshaw, S. E., & Dahlgren, R. A. (2012). Dissolved nitrous oxide concentrations and fluxes from the Eutrophic San Joaquin River, California. *Environmental Science & Technology*, *47*, 1313–1322. https://doi.org/10.1021/es301373h

Hotchkiss, E. R., Hall, R. O., Jr, Sponseller, R. A., Butman, D., Klaminder, J., Laudon, H., et al. (2015). Sources of and processes controlling CO2 emissions change with the size of streams and rivers. *Nature Geoscience*, *8*, 696–699. https://doi.org/10.1038/NGEO2507

Kaushal, S. S., Mayer, P. M., Vidon, P. G., Smith, R. M., Pennino, M. J., Newcomer, T. A., et al. (2014). Land use and climate variability amplify carbon, nutrient, and contaminant pulses: A review with management implications. *Journal of the American Water Resources Association*, *50*, 585–614. https://doi.org/10.1111/jawr.12204

Koffler, D., & Laaha, G. (2012). LFSTAT- an R-package for low-flow analysis. Retrieved from http://cra

Kyllmar, K., Carlsson, C., Gustafson, A., Ulén, B., & Johnsson, H. (2006). Nutrient discharge from small agricultural catchments in Sweden: Characterization and trends. *Agriculture, Ecosystems & Environment*, *115*, 15–26. https://doi.org/10.1016/j.agee.2005.12.004

Levi, L., Cvetkovic, V., & Destouni, G. (2018). Data-driven analysis of nutrient inputs and transfers through nested catchments. *The Science of the Total Environment*, *610–611*, 482–494. https://doi.org/10.1016/j.scitotenv.2017.08.003

Marinos, R. E., Van Meter, K. J., & Basu, N. B. (2020). Is the river a chemostat?: Scale versus land use controls on nitrate concentration-discharge dynamics in the upper Mississippi river basin. *Geophysical Research Letters*, *47*, 1–11. https://doi.org/10.1029/2020GL087051

Marzadri, A., Amatulli, G., Tonina, D., Bellin, A., Shen, L. Q., Allen, G. H., et al. (2021). Global riverine nitrous oxide emissions: The role of small streams and large rivers. *The Science of the Total Environment*, *776*, 145148. https://doi.org/10.1016/j.scitotenv.2021.145148

Marzadri, A., Dee, M. M., Tonina, D., Bellin, A., & Tank, J. L. (2017). Role of surface and subsurface processes in scaling N2O emissions along riverine networks. *Proceedings of the National Academy of Science of the United States of America*, *114*, 4330–4335.

Miller, O. L., Putman, A. L., Alder, J., Miller, M., Jones, D. K., & Wise, D. R. (2021). Changing climate drives future streamflow declines and challenges in meeting water demand across the southwestern United States. *Journal of Hydrology X*, *11*, 100074. https://doi.org/10.1016/j.hydroa.2021.100074

Montgomery, D. R., & Buffington, J. M. (1998). Channel processes, classification, and response. In R. J. Naiman, & R. Bilby (Eds.), *River ecology and management* (pp. 13–42). Springer-Verlag.New York.

Mosley, L. M. (2015). Drought impacts on the water quality of freshwater systems; review and integration. *Earth-Science Reviews*, *140*, 203–214. https://doi.org/10.1016/j.earscirev.2014.11.010

Mulholland, P. J., Helton, A. M., Poole, G. C., Hall, R. O., Hamilton, S. K., Peterson, B. J., et al. (2008). Stream denitrification across biomes and its response to anthropogenic nitrate loading. *Nature*, *452*, 202–205. https://doi.org/10.1038/nature06686

Overpeck, J. T. (2013). The challenge of hot drought. *Nature*, *503*, 350–351.

Peterson, E. E., & Ver Hoef, J. M. (2014). STARS: An ArcGIS toolset used to calculate the spatial information needed to fit spatial statistical models to stream network data. *Journal of Statistical Software*, *56*, 1–17. https://doi.org/10.18637/jss.v056.i02

Piccolroaz, S., Di Lazzaro, M., Zarlenga, A., Majone, B., Bellin, A., & Fiori, A. (2016). HYPERstream: A multi-scale framework for streamflow routing in large-scale hydrological model. *Hydrology and Earth System Sciences*, *20*, 2047–2061. https://doi.org/10.5194/hess-20-2047-2016

Ravishankara, A. R., Daniel, J. S., & Portmann, R. W. (2009). Nitrous oxide (N2O): The dominant ozone-depleting substance emitted in the 21st century. *Science*, *326*, 123–125. https://doi.org/10.1126/science.1176985

Rinaldo, A., Botter, G., Bertuzzo, E., Uccelli, A., Settin, T., & Marani, M. (2006). Transport at basin scales: 1. Theoretical framework. *Hydrology and Earth System Sciences*, *10*, 19–29.

Rutherford, J. C. (1994). *River mixing*. John Wiley & Sons.

Salarashayeri, A. F., & Siosemarde, M. (2012). Prediction of soil hydraulic conductivity from particle-size distribution. *World Acadmey of Science Engineering and Technolnology*, *61*, 454–458.

Seitzinger, S. P. (1988). Denitrification in freshwater and coastal marine ecosystems: Ecological and geochemical significance. *Limnology & Oceanography*, *33*, 702–724. https://doi.org/10.4319/lo.1988.33.4_part_2.0702

Seitzinger, S. P., Kroeze, C., & Styles, R. V. (2000). Global distribution of N2O emissions from aquatic systems: Natural emissions and anthropogenic effects. *Chemosphere - Global Change Science*, *2*, 267–279. https://doi.org/10.1016/S1465-9972(00)00015-5

Sheffield, J., Wood, E. F., Chaney, N., Guan, K., Sadri, S., Yuan, X., et al. (2014). A drought monitoring and forecasting system for sub-sahara african water resources and food security. *Bulletin of the American Meteorological Society*, *95*, 861–882. https://doi.org/10.1175/BAMS-D-12-00124.1

Smakhtin, V. U. (2001). Low flow hydrology: A review. *Journal of Hydrol.*, *240*, 147–186.

Stewart, R. J., Wollheim, W. M., Gooseff, M. N., Briggs, M. A., Jacobs, J. M., Peterson, B. J., et al. (2011). Separation of river network–scale nitrogen removal among the main channel and two transient storage compartments. *Water Resoure Research*, *47*, W00J10.

Tonina, D., Marzadri, A., Alberto, B., Deed, M., Bernal, S., & Tank, J. (2021). *Data: Riverine N_2O emissions from drying streams and rivers, HydroShare*. Retrieved from http://www.hydroshare.org/resource/70a1078d0ca14839aeea8e0f4082cb81

Tubino, M. (1991). Growth of alternate bars in unsteady flow. *Water Resource Research*, *27*, 37–52.

Turner, P. A., Griffis, T. J., Lee, X., Baker, J. C., Venterea, R. T., & Wood, J. C. (2015). Indirect nitrous oxide emissions from streams within the US Corn Belt scale with stream order. *Proceedings of the National Academy of Sciences of the United States of America*, *112*(32), 9839–9843. https://doi.org/10.1073/pnas.1503

Ver Hoef, J. M., Peterson, E. E., Clifford, D., & Shah, R. (2014). SSN: An R package for spatial statistical modeling on stream networks. *Journal of Statistical Software*, *56*, 1–45. https://doi.org/10.18637/jss.v056.i03

Vidon, P. G., & Cuadra, P. E. (2010). Impact of precipitation characteristics on soil hydrology in tile-drained landscapes. *Hydrological Processes*, *24*, 1821–1833. https://doi.org/10.1002/hyp.7627

WMO. (2008). *Manual on low-flow estimation and prediction: Operational hydrology report no. 50 WMO-No. 1029*.

Yalin, M. S. (1964). Geometrical properties of sand waves. *Proceedings of American Society of Civil Engineers, Journal of Hydraulics Division*, *90*, 105–119.

References From the Supporting Information

Elliott, A. H., & Brooks, N. H. (1997). Transfer of nonsorbing solutes to a streambed with bed forms: Theory. *Water Resoure Research*, *33*, 123–136. https://doi.org/10.1029/96WR02784

Gillihan, T. (2013). *Dynamic vegetation roughness in the riparian zone*. University of New Mexico.

Jähne, B., Münnich, K. O., Bösinger, R., Dutzi, A., Huber, W., & Libner, P. (1987). On the parameters influencing air-water gas exchange. *Journal of Geophysical Research*, *92*(C2), 1937–1949. https://doi.org/10.1029/JC092iC02p01937

Ikeda, S. (1984). Prediction of alternate bar wavelenght and height. *Journal of Hydraulic Engineering 110*, 371–386.

Leopold, L. B., & Maddock, T. (1953). *The hydraulic geometry of stream channels and some physiographic implications*.

Marineau, M., Wright, S. A., Whealdon-Haught, D. R., & Kinzel, P. J. (2017). *Physical characteristics of the lower san Joaquin River, California, in relation to white sturgeon spawning scientific investigations. Report 2017 – 5069*. https://doi.org/10.3133/sir20175069

Marzadri, A., Tonina, D., & Bellin, A. (2020). Power law scaling model predicts N_2O emissions along the Upper Mississippi River basin. *The Science of the Total Environment*, *732*, 138390. https://doi.org/10.1016/j.scitotenv.2020.138390

Raymond, P. A., Zappa, C. J., Butman, D., Bott, T. L., Potter, J., Mulholland, P. J., et al. (2012). Scaling the gas transfer velocity and hydraulic geometry in streams and small rivers. *Limnology & Oceanography*, *2*, 41–53. https://doi.org/10.1215/21573689-1597669

Wanninkhof, R. (1992). Relation between wind speed and gas exchange over the ocean. *Journal of Geophysical Research 97*, 7373–7382. https://doi.org/10.1029/92JC00188

Zambrano-Bigiarini, M. (2020). *hzambran/hydroGOF: v0.4-0*. https://doi.org/10.5281/ZENODO.3707013